

Characterization, Antibacterial and Antioxidant of Phytosynthesized Zinc Oxide Nanoparticles Using *Aloe Fleurentinorum* Leaves Extract

Yasmin M.S. Jamil¹ *, Hussein M.A. Al-Maydama¹, Ahmed N. Al-Hakimi², Ghadeer Y.S. Al-Mahwiti¹, Hassan M. Ibrahim³ and Basem Al-Akhali³

¹Department of Chemistry, Faculty of Science, Sana'a 12231 University, Sana'a, Yemen,

²Department of Chemistry, Faculty of Science, Ibb University, Ibb, Yemen,

³Biological Science Department, Faculty of Science, Sana'a University, Sana'a 12231, Yemen

*Corresponding author: y.jamil@su.edu.ye ; yasminjml@yahoo.com

ABSTRACT

The environmentally friendly methods for synthesizing metal oxide nanoparticles effectively save time, money, and effort. These methods involve the phytosynthesis process, which depends on plant extracts. To produce zinc oxide nanoparticles ($ZnO - NP_s$), we used at this work an extract of *Aloe Fleurentinorum* Leaves (AFL) as a reducing, capping, and stabilizing agent. As well as the effect of altering some parameters on the synthesis of $ZnO - NP_s$, such as the Temperature (T), the potential of hydrogen (pH), and the volume ratio (V/V), was studied using an X-ray diffractometer (XRD), crystallite size, and microstrain was determined, and the average crystallite size was between 16.50, and 25.99 nm. Also, $ZnO - NP_s$ were characterized optically by a UV-Vis spectrophotometer and got 3.13 eV band gap energy. Fourier transfer infrared spectroscopy was used for characterization. The antibacterial activities of $ZnO - NP_s$ were investigated against four bacterial species, and the results exhibit a noticeable effect, especially against gram-positive species, with inhibition zones ranging from 17 to 20 mm for the different concentrations. Also, the DPPH free radical method was used to evaluate the antioxidant properties of the synthesized zinc oxide nanoparticles at various concentrations, which showed a moderate scavenging efficiency of 52.74% at 800 $\mu\text{g/mL}$.

ARTICLE INFO

Keywords:

Green Synthesis
, ZnO Nanoparticles
, *Aloe Fleurentinorum*
, Antibacterial
, Antioxidant

Article History:

Received: 14-June-2024,
Revised: 28-July-2024,
Accepted: 10-August-2024,
Available online: 30 August 2024.

1. INTRODUCTION

Nanomaterial research has been developing rapidly and has potential in various fields, including biomedicine, magnetic sciences, biosensors, optoelectronics catalysis [1–3], electrical [4], antibacterial [5], and optical properties [6]. The nanomaterials are used in a variety of applications in the biomedical, and pharmaceutical industries. Metallic oxide nanoparticles such as ZnO have been studied for their antibacterial activity. That is because of the advancement of nanotechnology in synthesizing these particles on a nanometer scale, allowing them to interact with a variety of microorganisms [7]. Recently, metal oxide nanoparticles of copper, zinc, iron, Nickel [8], and cerium oxide have attracted attention owing to

their unique biological, chemical, and physical properties [9]. Zinc oxide nanoparticles ($ZnO - NP_s$) are important metal oxides for their interesting properties and wide applications in various fields. Nanosized ZnO particles are an important inorganic semiconductor material with a hexagonal wurtzite crystal structure, which has a wide, and direct b, and gap (3.36 eV), and a large excitonic binding energy (60 m eV)at ambient temperature [10–12]. There are numerous reports on the synthesis of ZnO nanoparticles using different methodological approaches like precipitation, laser ablation, sol-gel, methods polymerization method, [11] solvothermal, and hydrothermal synthesis [11–13]. These techniques have several drawbacks but the use of environmentally friendly synthesis

techniques will be capable of making $ZnO - NP_s$ the material as the plant-based synthesis. Plants and their extracts are simple to obtain, and the requirement for the procedure is a zinc salt solution which acts as a precursor metal. Fascinatingly, the morphological parameters of nanoparticles (size & shape) can be modulated by varying concentrations of procure material, and reaction conditions (temperature & pH) [14]. Various works on the use of plant extract to synthesize $ZnO - NP_s$ have been reported. Aloe plant is a cactus-like plant since it is succulent, has thorns along the edge of its leaves, is covered with wax, and contains a lot of water [1]. From the 20 species of Aloe L. genus presented in Yemen, Aloe Fleurentinorum Lavranos, and Newton [15, 16], which used in this study to prepare ZnO-NPs by the green approach. This work aims to synthesize $ZnO - NP_s$ via a green process using the natural extracts of Aloe Fleurentinorum leaves (AFL), study the structural properties using the XRD technique, examine the antibacterial potency against strains of pathogenic bacteria, and study their antioxidant efficiency.

2. EXPERIMENTAL

2.1. CHEMICALS AND MATERIALS

Zinc nitrate ($Zn(NO_3)_2 \cdot 6H_2O$; BDH (England)), Ammonia solution, absolute ethanol, methanol, DMSO solvent, DPPH free radicals agent, deionized water from a science college laboratory, and Aloe Fleurentinorum plant leaves were collected at summertime of 2022.

2.2. CHARACTERIZATIONS

A METROHM pH meter is used to adjust the synthesis's pH values. The effect of conditions variation of nanoparticle synthesis was observed, and crystalline properties were studied by XD-2 (Shimadzu ED-720) powder X-ray diffractometer at a voltage of 36 kV, and a current of 20 mA using $CuK(\alpha)$ radiation in the range of $5^\circ < 2\theta < 75^\circ$ a wavelength of 1.54056 \AA at 1° min^{-1} scanning rate. A SPECTROD200 (analytikjena) Ultraviolet, and Visible double-beam spectrophotometer used with a wavelength range from 300 to 700 nm was used for studying the optical properties of the synthesized $ZnO - NP_s$. The molecules, present as the nanoparticles' capping reduction agent were characterized using Fourier transform infrared (FTIR), which was used from a 400 to 4000 cm^{-1} range of wavenumber.

2.3. METHODS

2.3.1. The Preparation of Aloe Fleurentinorum Plant Extract

The Aloe Fleurentinorum leaves were presented from Dr Hassan Ibrahim Garden, Sana'a, Yemen. The leaves were washed several times with distilled water. Then,

dried at room temperature for three days away from sunlight, the dried leaves ground to fine powder. Then, 5 g of the powdered plant was immersed in 100 mL deionized water, and stirred using a magnetic stirrer for 30 min. at 60°C ; then the extract was cooled at room temperature, filtered, and saved at 4°C in the refrigerator [17].

2.3.2. $ZnO - NP_s$ green synthesis

A 0.202 M of Zinc nitrate was prepared by dissolving 6 gm of $Zn(NO_3)_2 \cdot 6H_2O$ in 100 mL deionized water, and the aqueous AFL extract was added to $Zn(NO_3)_2 \cdot 6H_2O$ solution with different reaction conditions to study the effect of these conditions for the synthesis of ZnO-NPs.

2.3.2.1. Green synthesis at different volume ratios

Five volume ratios (1:1, 1:2, 1:3, 1:4, 1:5) solutions were prepared by mixing a fixed volume of AFL extract (10mL) with a certain volume of $Zn(NO_3)_2$ (0.202M), (10, 20, 30, 40, 50 mL); they were labeled with H_1 , H_2 , H_3 , H_4 , and H_5 , and the pH value of the reaction adjusted at 7 by diluted NH_3 solution at 23°C for two hours mixing using a magnetic stirrer. The resulting brown precipitate was collected via centrifugation, then washed several times with deionized water, and once with ethanol, and left to dry for two hours in a drying oven at 100°C . The resultant powder was calcined at 500°C for two hours in a furnace. The light-yellow powder of $ZnO - NP_s$ grounded into a fine powder and then stored for characterization.

2.3.2.2. Green synthesis at different pH mediums

By selection of a fixed volume ratio (1:5), four solutions were prepared (H_6 , H_7 , H_8 , H_9 , H_{10}) by changing the pH values of the reaction by adding diluted NH_3 solution at pH = 6, 7, 8, 9, and 10, and were mixed using a magnetic stirrer for two hours. Then the same previous steps were followed in extracting the ZnO-NPs precipitate.

2.3.2.3. Green synthesis at different temperatures

Using fixed values of volume ratio (1:5), and pH=8, five solutions were prepared at different temperatures (23, 40, 60, 80°C), and labeled as (H_{11} , H_{12} , H_{13} , H_{14}) for two hours mixing upon continuous stirring. Then the same previous steps were followed in extracting the Zinc Oxide nanoparticle precipitate.

2.3.3. Antibacterial activity of $ZnO - NP_s$

The antibacterial properties of the green synthesized $ZnO - NP_s$ were assessed using an agar well diffusion method [18] against four bacterial pathogens. Gram-positive (Staphylococcus aureus; Bacillus Subtilis), and gram-negative (Escherichia coli; Salmonella typhi) bacterial colonies were cultured in nutrient broth at 37°C for 24 h. In this test the bacterial cells were inoculated on Petri dishes then we made holes in the bacterial dishes. Four concentrations of the $ZnO - NP_s$ suspension (4, 2, 1, and 0.5 mg/mL) were prepared by dis-

persing the required amount of $ZnO - NP_s$ in dimethyl sulfoxide DMSO, which were labeled as (Z_{10} , Z_{11} , Z_{12} , Z_{13} , respectively) for $ZnO - NP_s$ synthesized by AFL, respectively, and the antibiotic (Gentamycin, 2 mg/mL) was used as a positive control; the holes in Petri dishes which were made filled with the prepared solutions of $ZnO - NP_s$, and the positive control; then the dishes were incubated for 24 hours. The antibacterial activity of the samples was determined by measuring the inhibition zones around the samples in mm.

2.4. ANTIOXIDANT ACTIVITY OF ZnO-NPs USING DPPH METHOD

In this approach, The DPPH method has been used; 1,1-diphenyl-2-picryl hydrazyl (DPPH) solution was prepared in methanol and then incubated in the dark for 1h. Different concentrations of $ZnO - NP_s$ (0.8, 0.6, and 0.4 mg/mL) were prepared by suspending them in methanol; 1mL of these concentrations was added to 1mL of the freshly prepared DPPH solution separately, and mixed very well; then, the mixture was incubated in darkness for 30 min. The absorbance of the reaction mixture at 517 nm was read by the UV-Vis Spectrophotometer. All the experiments were performed in triplicate. Then, the percentage scavenging was calculated using equation 1.

$$\text{Scavenging}\% = \frac{A_o - A_s}{A_o} \times 100 \quad (1)$$

where A_o is the absorbance of the control group, and A_s is the absorbance of the sample

3. RESULTS AND DISCUSSION

3.1. PHYSIOCHEMICAL STUDIES OF GREEN SYNTHESIZED $ZnO - NP_s$ BY AFL

3.1.1. X-ray Diffraction studies for the synthesized ZnO nanoparticles at different conditions

3.1.1.1. The effect of the volume ratio of reactants

In the study, Zinc oxide Nanoparticles were synthesized using a fixed volume of AFL aqueous extract, and different volumes of (0.202M Zinc nitrate). XRD measurements for these resultant $ZnO - NP_s$ are shown in Figure 1. All the patterns obtained show similarity for the synthesized $ZnO - NP_s$ with the zincite phase of the standard card file (JCPDS-036-1451) and follow the spectra at diffraction lines (100), (002), (101), (102), (110), (103), (200), (112), (201), and (004). This shows that the $ZnO - NP_s$ have a hexagonal crystalline structure. The size of the formed nanoparticles was determined using two procedures: Debye–Scherrer's Equation "D-Sh" 2 [19], and Williamson–Hall's Equation "W-H" 3, the microstrain (ϵ) was determined using two procedures: Williamson–Hall's Equation 2, and Equation 4

and summarized in Table 1.

$$D_{d-sh} = \frac{k\lambda}{\beta \cos \theta} \quad (2)$$

$$\beta_{hkl} \cos \theta = \left(\frac{k\lambda}{D_{W-H}} \right) + 4\epsilon \sin \theta \quad (3)$$

Where D is the average particle size, K is a constant (0.94), λ is the wavelength of the x-ray ($1.5406A_o$), β is the full width at half maximum of the peak (FWHM), θ is the position of the diffraction peak, and ϵ is the microstrain which determined from Equation 3, and the slope from Equation 2 as shown in Figure 2.

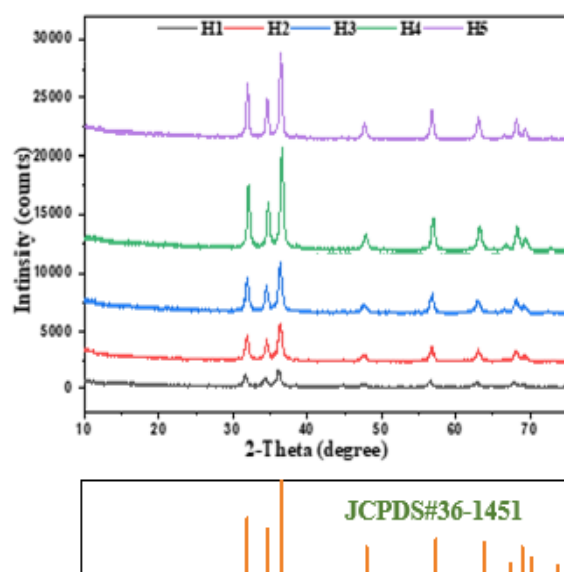


Figure 1. XRD patterns for synthesized $ZnO - NP_s$ at different volume ratios.

Table 1. The calculated particle size and microstrain at different pH.

PH	FWHM (degree)	D_{d-sh} (nm)	ϵ	D_{W-H} (nm)	ϵ_{W-H}
1:1	0.06	17.27	3.1×10^{-4}	16.52	5.3×10^{-3}
1:2	0.59	16.47	-1.1×10^{-4}	15.56	5.6×10^{-3}
1:3	0.55	17.35	1.6×10^{-4}	17.62	5.1×10^{-3}
1:4	0.46	20.31	-1.1×10^{-4}	19.65	4.4×10^{-3}
1:5	0.43	22.23	2.4×10^{-4}	23.57	4.0×10^{-3}

From Table 1 we observe that by increasing the volume of Zinc ions the particle size was increased, and decreasing β value; Figure 3 shows the relation between particle size and volume ratio.

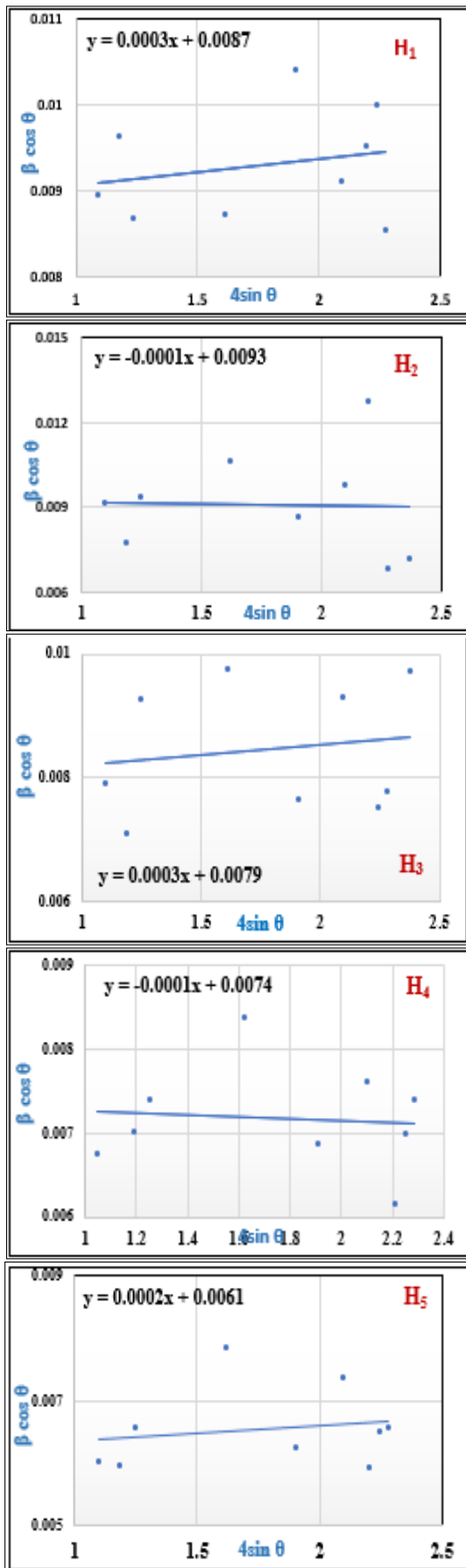


Figure 2. The W-H Equation patterns for synthesized $ZnO - NP_s$ at different pH

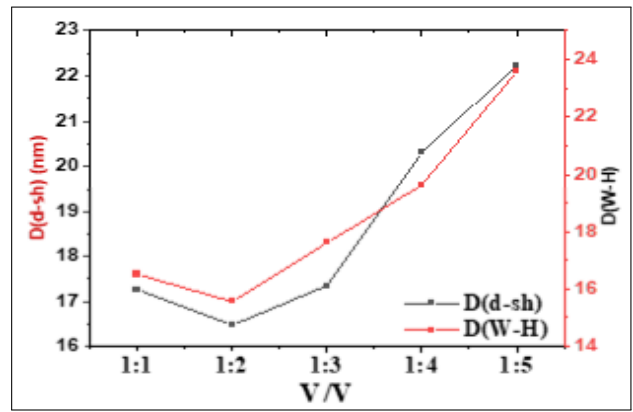


Figure 3. Relation between reactant pH value and particle size.

3.1.1.2. The effect of the pH value

In this section, zinc oxide Nanoparticles were synthesized at different pH mediums with a 1:5 volume ratio of reactants (the least β value) [7]; $ZnO - NP_s$ measurement of XRD is shown in Figure 4 that showed the peaks corresponding to the planes of hexagonal zincite (JCPDS-36-1451). The obtained particle size, and microstrain (ϵ) by Equations 2-4 are displayed in Table 1; pH=10 doesn't appear because the resultant dissolved at this value.

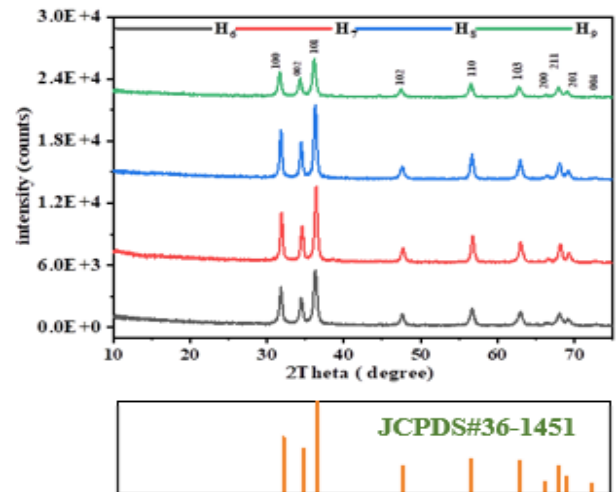


Figure 4. 4 XRD patterns for synthesized $ZnO - NP_s$ at different pH values.

Table 2. The calculated particle size and microstrain at different V/V .

V/V	FWHM (degree)	D_{d-sh} (nm)	ϵ	D_{W-H} (nm)	ϵ_{W-H}
6	0.51	18.45	5.4×10^{-4}	20.86	4.8×10^{-3}
7	0.43	22.23	2.4×10^{-4}	23.57	4.0×10^{-3}
8	0.39	25.99	3.6×10^{-4}	26.22	3.8×10^{-3}
9	0.52	18.29	3.0×10^{-4}	19.54	4.7×10^{-3}

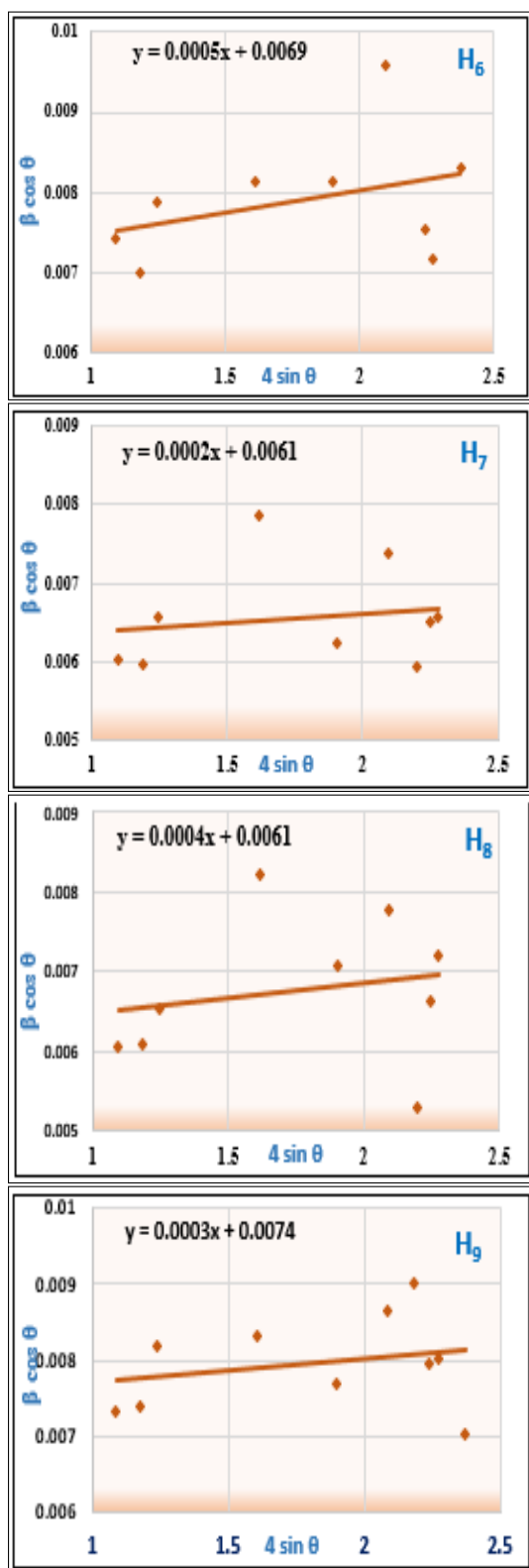


Figure 5. The W-H Equation patterns for synthesized ZnO-NPs at different V/V .

Table 2 showed an increase in particle size with pH increasing to 8, then decreasing at pH=9; Figure 5 likewise Figure 2 showed the patterns used to determine the particle size & microstrain by the W-H method; the effect of the variation in pH on the average particle size calculated by D-Sh, and W-H methods shown in Figure 6.

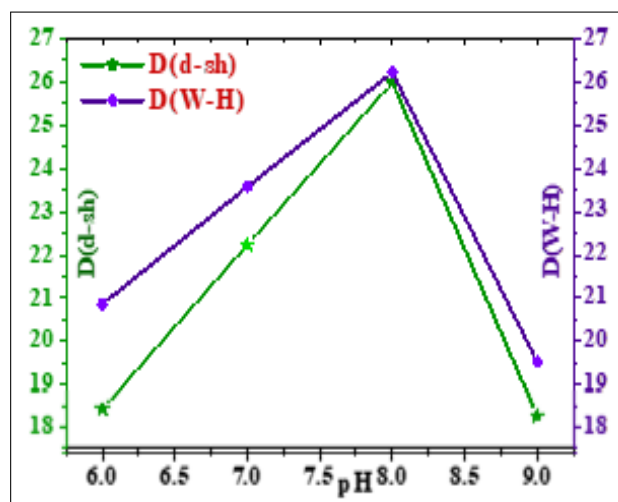


Figure 6. 4 XRD patterns for synthesized $ZnO - NP_s$ at different pH values.

3.1.1.3. The effect of the reaction temperature

For studying the effect of alteration in temperature of the reaction medium for $ZnO - NP_s$ synthesis (H_{11} , H_{12} , H_{13} , H_{14}) at 23, 40, 60, and 80 °C, respectively. Using the XRD analysis, we use a fixed volume ratio (1:5), and pH value = 8, which have the least average FWHM value. The XRD patterns of the synthesized $ZnO - NP_s$ are shown in Figure 7; Table 3 displays the obtained particle size, and microstrain (ϵ) calculated using Equations 2,3 and 4 respectively; Figure 8 shows the W-H Equation patterns for synthesized $ZnO - NP_s$ at different Temperature. It has been noticed that the smallest particle size was at $T=40$ °C, which has the highest FWHM value; Figure 9 shows the relation between Temperatures & particle size.

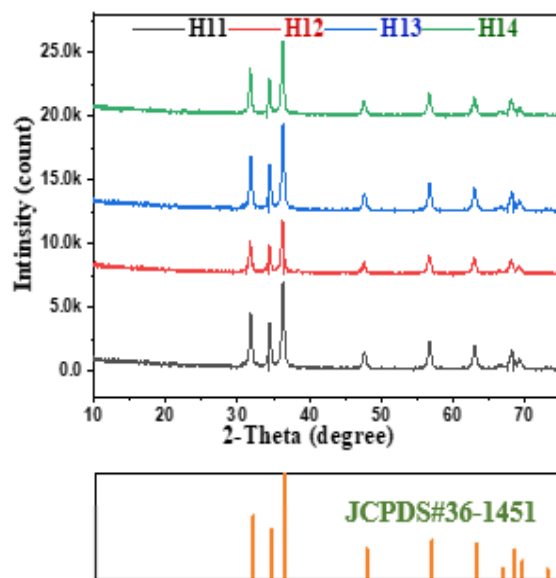


Figure 7. XRD patterns for synthesized ZnO-NPs at different Temperatures.

Table 3. The calculated particle size and microstrain at different Temperatures

T(°C)	FWHM (degree)	D_{d-sh} (nm)	ϵ	D_{W-H} (nm)	ϵ_{W-H}
23	0.39	25.99	3.6×10^{-4}	26.22	3.8×10^{-3}
40	0.74	21.47	1.5×10^{-3}	31.40	4.3×10^{-3}
60	0.44	23.76	2.8×10^{-5}	21.28	5.3×10^{-3}
80	0.43	22.60	1.5×10^{-4}	23.25	3.9×10^{-3}

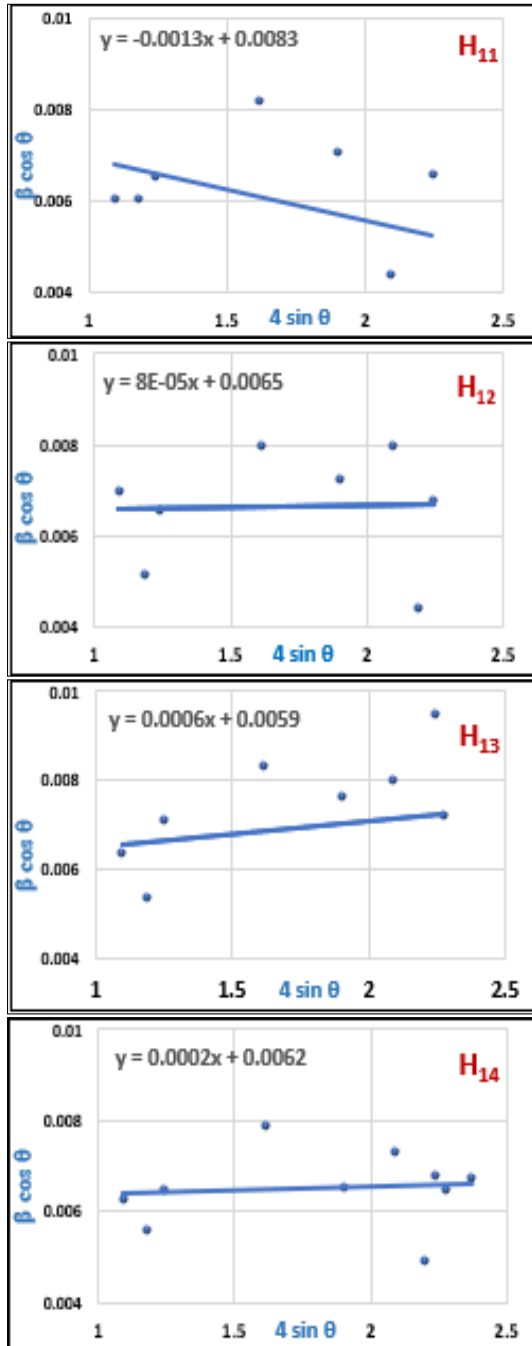


Figure 8. The W-H Equation patterns for synthesized ZnO-NPs at different T.

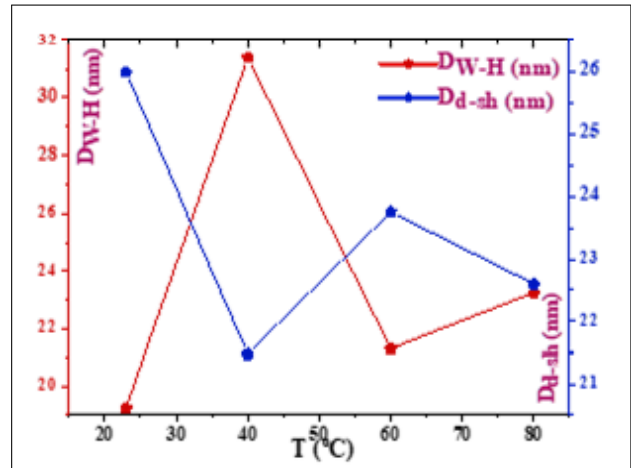


Figure 9. Relation between reactant Temperatures and particle size

3.1.2. UV-VIS Spectrometer studies for the synthesized by AFL.

UV-Vis spectrometry is a simple, and effective technique for determining the formation, shape, and consistency of nanoparticles in an aqueous solution; the most commonly used method for studying the optical properties of the particles is UV-Visible spectroscopy [20]; the zinc oxide nanoparticles optical absorbance spectra are shown in Figure 10; the band assigned to the absorption of zinc oxide nanoparticles was observed at 378 nm; a characteristic absorption peak at 378 nm was observed that could be related to ZnO intrinsic band gap absorption due to electron transfers from the valence b, and to the conduction b, and (O_{2p}/Zn_{3d}). This sharp peak shows that the particles are in Nano-size. The band gap energy of the ZnO nanoparticles was determined according to Tauc's plot method Equation 4 [21].

$$(\alpha h\nu)^2 = A \times (h\nu - E_g) \quad (4)$$

Where α is the absorption coefficient, $h\nu$ is the photon energy, h is the constant of the Plank (6.626×10^{-34} J.s), and E_g is the band gap Energy; the plotting of $(\alpha h\nu)^2$ as a function of photon energy, and extrapolating the liner portion of the curve to give the value of direct band gap is known as Tuac's plot; the ZnO nanoparticles band gap energy was 3.13 eV which was in good agreement with published [22, 23] .

3.1.3. FTIR Spectrophotometry studies for the synthesized ZnO-NPs by AFL

Figure 11 shows the FTIR spectra of the Aloe Fleurentinorum and ZnO nanoparticles calcined at 500 °C. A series of absorption peaks from 300 to 4000 cm^{-1} can be found, which correspond to the carboxylate, and hydroxyl groups in the extract sample. More specifically, the broadband at 3300 cm^{-1} was assigned to the O-H stretching mode of the hydroxyl group, and 1560 cm^{-1} for C=O which almost had been disappearing in ZnO

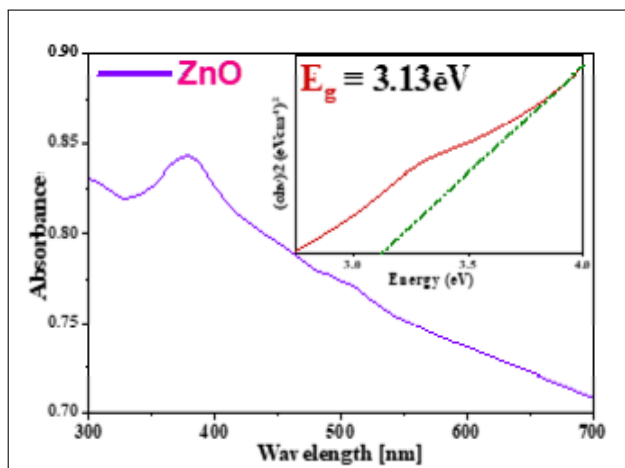


Figure 10. UV-vis spectrum and band gap estimation of synthesized $ZnO - NP_s$

spectra. The peak observed at 398 cm^{-1} is due to the hexagonal Zinc Oxide.

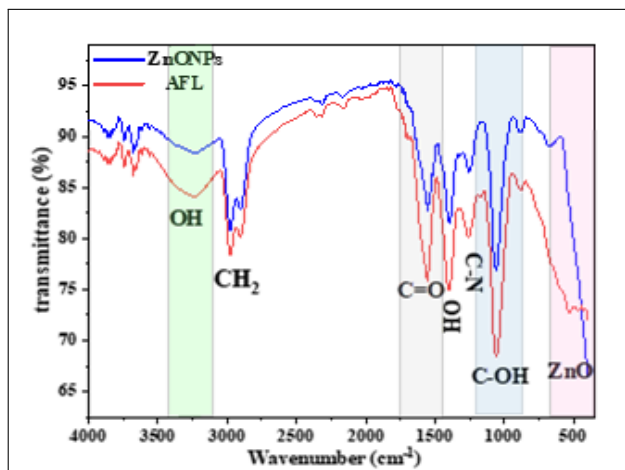


Figure 11. FTIR spectra of AFL extract and the synthesized $ZnO - NP_s$

3.2. ANTIBACTERIAL ACTIVITY OF ZNO NANOPARTICLES

The Antibacterial activity of the green synthesized ZnO nanoparticles using the extract of the Aloe Fleurentinorum leaves under the same conditions against two types of Gram (-) bacteria (*Salmonella Typhi*, and *Escherichia Coli*) and two species of Gram (+) bacteria (*Staphylococcus Aureus*, and *Bacillus Subtilis*). The activity of the four different concentrations of $ZnO - NP_s$ (Z_{10} , Z_{11} , Z_{12} , Z_{13}) was compared with standard Gentamycin antibiotics; the results exhibited a noticeable influence against the Gram (+) types of bacteria (17-20mm) more than the Gram (-) types (6-15.5mm). Figure 12 showed the highest effect was for the $ZnO - NP_s$ at 4mg/mL against Gram (+) *B. Subtilis* type; the higher effect against the Gram-positive bacteria compared to Gram-negative bacteria might be due to the Gram-positive bacteria being less susceptible

to antibacterial potency than Gram-negative bacteria; perhaps this is a result of their different cell wall structures [24]. In the Gram-positive strain, peptidoglycan is thick while being thinner in the Gram-negative, but contains an outer membrane lipopolysaccharide that provides the bacteria resistance to ZnO and makes them less susceptible [24, 25]. The $ZnO - NP_s$ and Gentamycin effect against all the bacteria types are shown in Figures 13 and 14, respectively.

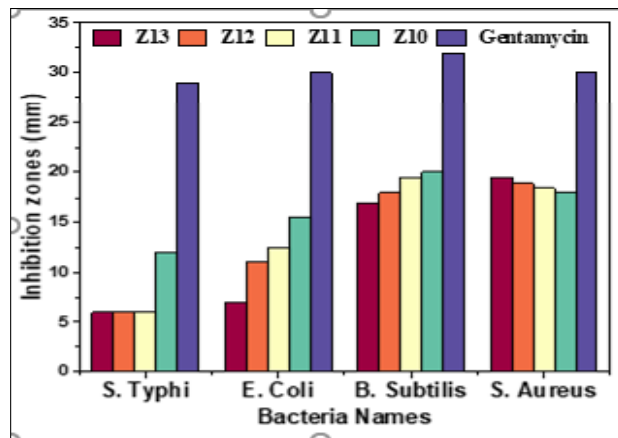


Figure 12. The Inhibition zones of green synthesized ZnO -NPs in different Concentrations.

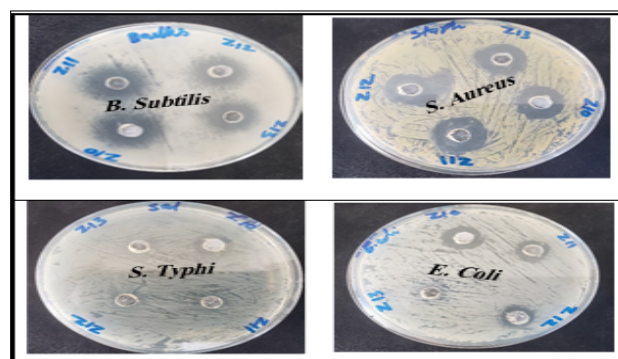


Figure 13. Antibacterial activity of ZnO -NPs against different bacterial types.

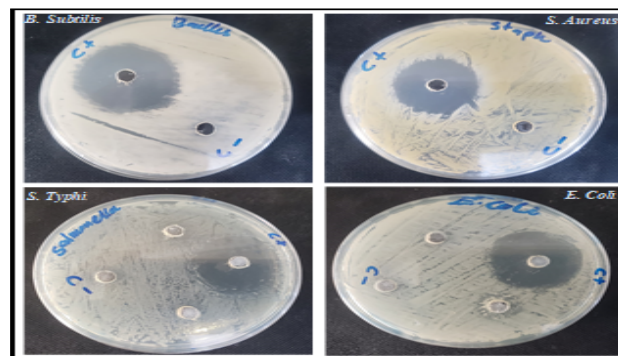


Figure 14. Gentamycin Antibacterial activity against different bacterial types.

3.3. ANTIOXIDANT ACTIVITY OF $ZnO - NPs$

The synthesized $ZnO - NPs$ antioxidant potential was investigated using the DPPH free radical assay, the widely recognized method for assessing antioxidant activity; $ZnO - NPs$ exhibited notable scavenging activity at various concentrations (400, 600, 800 $\mu\text{g/mL}$) Figure 15; the average determined percentage of scavenging of zinc oxide nanoparticles which was calculated by equation 1, ranging from 50.18 to 52.74%, and these are promising results.

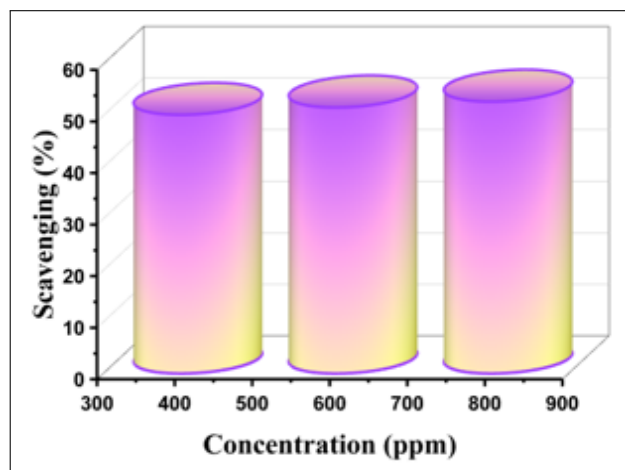


Figure 15. DPPH free radical scavenging activity for $ZnO - NPs$.

4. CONCLUSION

Zinc oxide nanoparticles have been synthesized successfully using the Phyto method by Aloe Fleurentinorum aqueous extract at different volume ratios, pH values, and temperature conditions. Whereas, X-ray diffraction shows the zincite phase had hexagonal structural, and crystallite size between (16.5 – 31.4 nm); the optical properties of $ZnO - NPs$ were studied by UV-Vis Spectrophotometry, and show energy band gap $E_g = 3.13\text{eV}$. The synthesized $ZnO - NPs$ showed an antibacterial activity to G(+) species better than G(-); furthermore, a noticeable Antioxidant property of $ZnO - NPs$ against the DPPH-free radicals was observed.

REFERENCES

- [1] N. I. Rasli, H. Basri, and Z. Harun, "Zinc oxide from aloe vera extract: Two-level factorial screening of biosynthesis parameters," *Heliyon*, vol. 6, no. 1, 2020. [Online]. Available: <https://doi.org/10.1016/j.heliyon.2020.e03156>.
- [2] V. Ravichandran, S. Vasanthi, S. Shalini, S. A. A. Shah, M. Tripathy, and N. Paliwal, "Green synthesis, characterization, antibacterial, antioxidant and photocatalytic activity of parkia speciosa leaves extract mediated silver nanoparticles," *Results Phys.*, vol. 15, p. 102565, 2019.
- [3] H. M. Al-Maydama, Y. M. Jamil, M. A. Awad, and A. A. Abduljabbar, "Electrochemical investigations and antimicrobial ac-

tivity of au nanoparticles photodeposited on titania nanoparticles," *Heliyon*, vol. 10, no. 1, 2024.

- [4] Y. M. Jamil, M. A. H. Awad, and H. M. Al-Maydama, "Electrochemical and catalytic properties of au nanoparticles,"
- [5] Y. M. Jamil, M. A. Awad, and H. M. Al-Maydama, "Physicochemical properties and antibacterial activity of pt nanoparticles on tio2 nanotubes as electrocatalyst for methanol oxidation reaction," *Results Chem.*, vol. 4, p. 100531, 2022. [Online]. Available: <https://doi.org/10.1016/j.rechem.2022.100531>.
- [6] A. Al-Hammadi, A. Al-Sharabi, and A. Alnehia, "Green and chemically prepared zinc sulfide nanoparticles: A comparative study," *Sana'a Univ. J. Appl. Sci. Technol.*, vol. 1, no. 1, 2023.
- [7] M. S. Osman et al., "Effective inhibition of waterborne and fungal pathogens using zno nanoparticles prepared from an aqueous extract of propolis: Optimum biosynthesis, characterization, and antimicrobial activity," *Appl. Nanosci.*, vol. 13, no. 6, pp. 4515–4526, 2023. [Online]. Available: <https://doi.org/10.1007/s13204-022-02726-w>.
- [8] Y. M. Jamil, M. A. H. Awad, H. M. Al-Maydama, Y. EL-Ghoul, and A. N. Al-Hakimi, "Synthesis and study of enhanced electrochemical properties of nio nanoparticles deposited on tio2 nanotubes," *Appl. Organomet. Chem.*, vol. 36, no. 9, e6795, 2022. [Online]. Available: <https://doi.org/10.1002/aoc.6795>.
- [9] S. Dönmez, "Green synthesis and characterization of zinc oxide nanoparticles by using rhododendron ponticum l. leaf extract," *Turkish J. Health Sci. Life*, vol. 4, no. 1, pp. 54–57, 2021.
- [10] R. M. Elsamra, M. S. Masoud, A. A. Zidan, G. M. E. Zokm, and M. A. Okbah, "Green synthesis of nanostructured zinc oxide by ocimum tenuiflorum extract: Characterization, adsorption modeling, cytotoxic screening, and metal ions adsorption applications," *Biomass Convers. Biorefinery*, vol. 14, no. 15, pp. 16843–16856, 2024. [Online]. Available: <https://doi.org/10.1007/s13399-022-03709-1>.
- [11] M. Darroudi, Z. Sabouri, R. K. Oskuee, A. K. Zak, H. Kargar, and M. H. N. Abd Hamid, "Green chemistry approach for the synthesis of zno nanopowders and their cytotoxic effects," *Ceram. Int.*, vol. 40, no. 3, pp. 4827–4831, 2014. [Online]. Available: <https://doi.org/10.1016/j.ceramint.2013.09.032>.
- [12] T. S. Aldeen, H. E. A. Mohamed, and M. Maaza, "Zno nanoparticles prepared via a green synthesis approach: Physical properties, photocatalytic and antibacterial activity," *J. Phys. Chem. Solids*, vol. 160, p. 110313, 2022. [Online]. Available: <https://doi.org/10.1016/j.jpccs.2021.110313>.
- [13] R. Razali, A. K. Zak, W. A. Majid, and M. Darroudi, "Solvothermal synthesis of microsphere zno nanostructures in dea media," *Ceram. Int.*, vol. 37, no. 8, pp. 3657–3663, 2011.
- [14] J. Singh, T. Dutta, K.-H. Kim, M. Rawat, P. Samddar, and P. Kumar, "Green synthesis of metals and their oxide nanoparticles: Applications for environmental remediation," *J. nanobiotechnology*, vol. 16, pp. 1–24, 2018. [Online]. Available: <https://doi.org/https://10.1186/s12951-018-0408-4>.
- [15] H. Ibrahim, Q. Abdullah, A. Humaid, A. Tabit, S. Al-alawi, and A. Al-ramsi, "Phytochemical screening and anti-microbial activities of aloe fleurentinorum lavranos & newton," *J. Chem. Biol. Phys. Sci.*, vol. 12, pp. 335–348, 2022. [Online]. Available: <https://doi.org/10.24214/jcbps.b.12.4.33548>.
- [16] A. W. A. Al-Khulaidi, A. H. Al-Qadasi, and O. S. S. Al-Hawshabi, "Natural plant species inventory of the important plant areas in arabian peninsula: Bani omar, taiz governorate, republic of yemen," *Electron. J. Univ. Aden for Basic Appl. Sci.*, vol. 1, no. 3, pp. 135–150, 2020. [Online]. Available: <https://doi.org/10.47372/ejua-ba.2020.3.36>.



- [17] Y. M. Jamil, A. N. Al-Hakimi, H. M. Al-Maydama, G. Y. Almahwiti, A. Qasem, and S. M. Saleh, "Optimum green synthesis, characterization, and antibacterial activity of silver nanoparticles prepared from an extract of aloe fleurentinorum," *Int. J. Chem. Eng.*, vol. 2024, no. 1, p. 2804165, 2024. [Online]. Available: <https://doi.org/10.1155/2024/2804165%20Research..>
- [18] Y. M. Jamil, F. M. Al-Azab, N. A. Al-Selwi, A. M. AL-Ryami, and M. R. Mlahia, "Spectroscopic and biological studies of mixed ligand complexes of transition metal (ii) ions with chloroquine and ketoprofen," *Sana'a Univ. J. Appl. Sci. Technol.*, vol. 2, no. 1, pp. 53–64, 2024. [Online]. Available: <https://doi.org/10.59628/jast.v2i1.801..>
- [19] Y. M. Jamil, "Synthesis and spectroscopic methods on the complexation of coii, niini and cuini," *Sana'a Univ. J. Appl. Sci. Technol.*, vol. 1, no. 1, 2023.
- [20] S. Ravichandran, J. Radhakrishnan, P. Sengodan, R. Rajendran, R. Ramalingam, and K. D. Arunachalam, "Bio synthesis of zinc oxide nanoparticles using clerodendrum phlomidis extract for antibacterial, anticancer, antioxidant and photocatalytic studies," *J. Mater. Sci. Mater. Electron.*, vol. 33, no. 14, pp. 11455–11466, 2022. [Online]. Available: <https://doi.org/10.1007/s10854-022-08118-8..>
- [21] S. Bissa, P. Naruka, R. Birthlya, and A. Jain, "Plant based synthesis of zno nanoparticles and characterization by uv-vis spectroscopy," *J. Condens. Matter. Vol*, vol. 1, no. 1, p. 46, 2023. [Online]. Available: <https://doi.org/10.61343/jcm.v1i01.9..>
- [22] M. Farag, S. M. El-Dafrawy, and S. M. Hassan, "Zno and c/zno catalysts synthesized via plant mediated extracts for photodegradation of crystal violet and methyl orange dyes," *J. Inorg. Organomet. Polym. Mater.*, vol. 34, no. 3, pp. 930–943, 2024. [Online]. Available: <https://doi.org/10.1007/s10904-023-02811-9..>
- [23] N. Kamarulzaman, M. F. Kasim, and R. Rusdi, "Band gap narrowing and widening of zno nanostructures and doped materials," *Nanoscale research letters*, vol. 10, pp. 1–12, 2015. [Online]. Available: <https://doi.org/10.1186/%20s11671-015-1034-9..>
- [24] A. Alnehia, A.-B. Al-Odayni, A. Al-Sharabi, A. Al-Hammadi, and W. S. Saeed, "Pomegranate peel extract-mediated green synthesis of zno-nps: Extract concentration-dependent structure, optical, and antibacterial activity," *J. Chem.*, vol. 2022, no. 1, p. 9647793, 2022. [Online]. Available: <https://doi.org/10.1155/2022/9647793..>
- [25] A. Rahman, M. H. Harunsani, A. L. Tan, N. Ahmad, B.-K. Min, and M. M. Khan, "Influence of mg and cu dual-doping on phyto-genic synthesized zno for light induced antibacterial and radical scavenging activities," *Mater. Sci. Semicond. Process.*, vol. 128, p. 105761, 2021.